

## Structural Response of BaTiO<sub>3</sub>/CaTiO<sub>3</sub> Superlattice to Applied Electric Fields

Ji Young Jo<sup>1</sup>, Rebecca J. Sichel<sup>1</sup>, Ho Nyung Lee<sup>2</sup>, Eric Dufresne<sup>3</sup>, and Paul G. Evans<sup>1</sup>

<sup>1</sup>Department of Materials Science and Engineering and Materials Science Program, University of Wisconsin-Madison, WI 53706, U.S.A.

<sup>2</sup>Materials Science and Technology Division, Oak Ridge National Laboratory, Oak Ridge, TN 37831, U.S.A.

<sup>3</sup>Advanced Photon Source, Argonne National Laboratory, Argonne, IL 60439, U.S.A.

### ABSTRACT

The structural response of a ferroelectric BaTiO<sub>3</sub>/dielectric CaTiO<sub>3</sub> superlattice to the bipolar applied electric field was studied using time-resolved x-ray microdiffraction. Structural results were compared to the polarization-electric field hysteresis curve obtained from electrical measurements. The superlattice x-ray reflections were found to have a broad distribution of intensity in reciprocal space under applied electric fields exceeding the nominal coercive electric field. The broad distribution of the lattice constant at high electric fields is compared with a model in which the constituent layers of the superlattice have different coercive fields for the polarization switching.

### INTRODUCTION

Ferroelectric/dielectric superlattices can be designed to control the polarization of their dielectric components using the electrostatic boundary conditions at the interfaces [1]. The lattice constant of superlattices is electromechanically coupled to the polarization, and depends on the electrostatic state of the superlattice [2]. The structural and electrical properties of the superlattice at zero external electric field have been well established both experimentally [3] and theoretically [4] based on the electrostatic energy argument. How both the overall polarization and the lattice parameter of the superlattice response to applied electric fields, however, remains an important open question.

The polarization switching process in the superlattice is affected by the electrostatic energy of neighboring domains with differing polarization states. Nano-scale domain can form within superlattices due to the bound charge at interfaces [5]. Polarization switching results in a coupling between the structural properties and the polarization because the lattice distortion is proportional to electric polarization [6]. By probing the structural and electrical properties of a superlattice during polarization switching we obtain insight into how these electrostatic conditions vary in applied electric fields. Here we combine *in-situ* studies of lattice distortion and electrical displacement current measurements for a ferroelectric/dielectric superlattice capacitor in applied electric fields. A broad distribution of lattice constant was found in electric field region higher than the nominal coercive field.

## EXPERIMENT

Each period of the superlattice for this study consisted of 2 unit cells of ferroelectric BaTiO<sub>3</sub> and 4 unit cells of dielectric CaTiO<sub>3</sub>. The superlattice thin film with a nominal thickness of 200 nm was deposited on a 4 nm-thick SrRuO<sub>3</sub> bottom electrode on a SrTiO<sub>3</sub> substrate by using pulsed laser deposition [2]. External electric fields were applied using a conducting tip to contact a Pt top electrode with a diameter of 100 μm. X-ray experiments were conducted with a photon energy of 10 keV at station 7ID of the Advanced Photon Source. To measure lattice constant of the superlattice thin film under applied electric fields, x-rays were focused using a Fresnel zone plate to a 300 nm spot located within the region covered by the top electrode of a capacitor [7]. A triangular wave electric field with 5 ms duration was applied across the capacitor, and the diffracted intensity was simultaneously measured using an avalanche photodiode detector. A time resolved measurement of the intensity was obtained by sorting the signal from the detector into 500 channels, each with a dwell time of 10 μs, using a multi-channel scaler.

In superlattices, x-ray satellite reflections due to the periodic structure appear at

$$2 \frac{\sin \theta}{\lambda} = \frac{m}{t_0} + \frac{l}{\Lambda},$$

where  $l$  is an integer that labels the order of satellite around the main Bragg peak indexed with an integer  $m$  and  $t_0$  is an average lattice parameter in a period with total thickness of  $\Lambda$ . At zero external electric field, the value of  $t_0$  obtained from the reflection at  $m=2$   $l=0$  is 3.985 Å.  $\theta$  is the incident angle with respect to the lattice planes of the superlattice and  $\lambda$  is the x-ray wavelength, 1.238 Å for a photon energy of 10 keV.

Polarization-electric field hysteresis loops were measured by applying the same triangular wave electric field used for the *in-situ* x-ray measurements. The current through a 50 Ω resistor in series with a capacitor was recorded using an oscilloscope. The measured current consisted of the switching current and the polynomial current-voltage term due to a leakage current [8]. This contribution from a leakage current was fitted with polynomial current-voltage function and then subtracted from the measured current. The polarization as a function of electric field plotted in Fig. 1 was obtained by integrating the electrical displacement current. The effect of the contribution from the leakage current was checked by comparing the polarization-electric field hysteresis loops before and after subtracting the leakage current. The coercive field values changed from 0.2 and -0.4 MV/cm to approximately 0.1 and -0.3 MV/cm for positive and negative electric field directions. The remnant polarization value changed from 17 μC/cm<sup>2</sup> to approximately 10 μC/cm<sup>2</sup>.

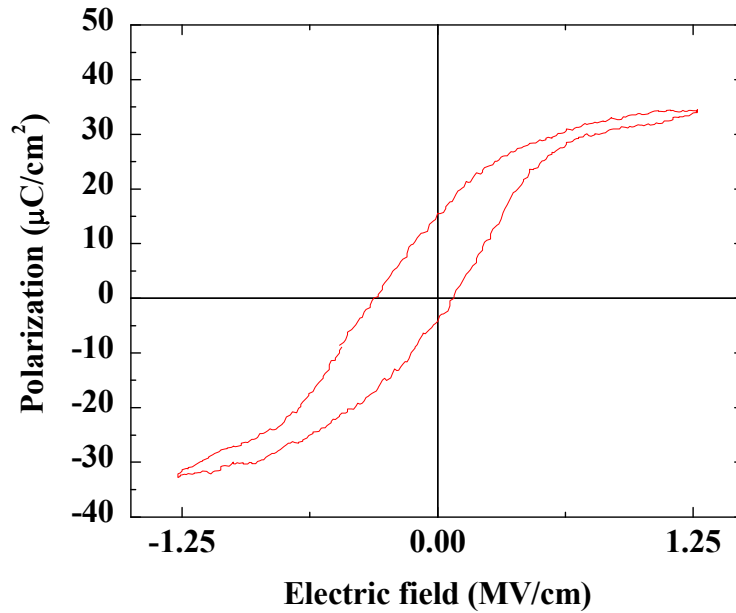


**Figure 1.** Polarization-electric field hysteresis loop for the superlattice capacitor, acquired using a 5 ms triangle-wave electric field pulse. Current arising from leakage has been subtracted using polynomial fit.

## DISCUSSION

The shift of reflections with applied electric fields can be used to determine both the lattice constant and the direction of the stored polarization with respect to the applied electric field. The  $\theta$  angle of the maximum intensity of the  $m=2$   $l=0$  reflection shifts to lower values in applied electric fields because the lattice parameter of the superlattice increases due to piezoelectric expansion. This effect is shown for a bipolar electric field in Fig. 2. At fields higher than the coercive electric fields of the superlattice, the polarization of the superlattice is parallel to the applied electric field, resulting in the observed increase of the lattice constant.

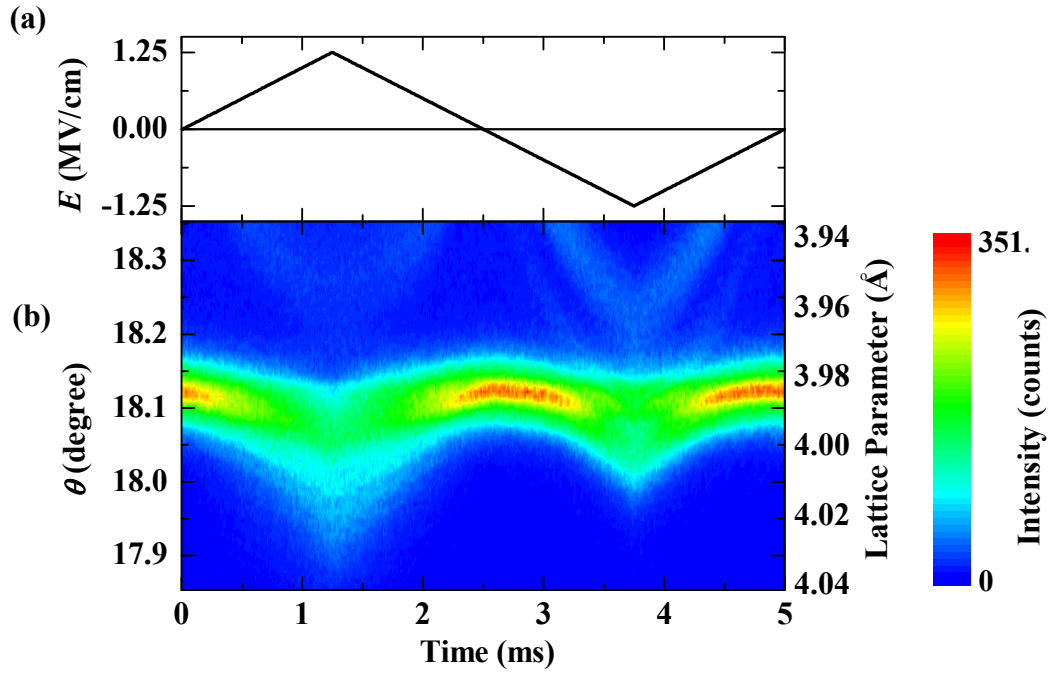


**Figure 2.** (a) Applied electric field  $E$  and (b) diffracted x-ray intensity at the  $m=2$   $l=0$  reflection of superlattice under the applied electric field.

To obtain more information about the structural properties of the superlattice under applied electric fields, we fit the distribution of intensity at the  $m=2$   $l=0$  satellite reflection with a sum of multiple Gaussian functions. These contributions are shown with the series of dashed, dotted, and dashed dotted lines in Fig. 3. The sum of all three sub-peaks is shown as the solid line in Fig. 3. The two main sub-peaks have intuitive origins, arising from contributions from two separate reflections indexed as  $m=2$   $l=0$ . A third reflection represents the contribution of adjacent reflection. The splitting of these reflections may arise from slight inhomogeneity of the response of the superlattice across the 80 periods of its thickness.

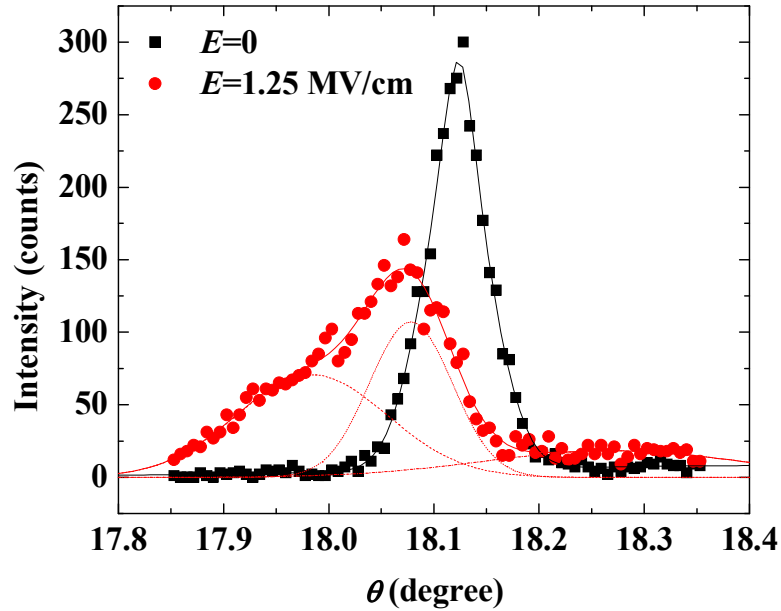


**Figure 3.** Intensity distribution at the  $m=2l=0$  reflection when (solid square)  $E=0$  and (solid circle)  $E=1.25$  MV/cm. The dashed, dotted, and dashed-dotted lines represent three Gaussian functions used to fit the experimentally observed intensity (solid symbols). The solid line is the sum of the fitting functions.

The lattice distortion of the superlattice at the positive electric field is larger than that at negative electric field, as shown in Fig. 2(b). The large distortion at positive fields arises because the polarization domains favor alignment in the positive field direction, as is evident from the polarization. The low distortion at negative fields may also indicate that the superlattice is incompletely switched into the negative polarization state. We have observed a similar effect in incompletely switched  $\text{Pb}(\text{Zr},\text{Ti})\text{O}_3$  thin films [7]. There is no sharp transition of piezoelectric lattice distortion, either in the polarization-electric field hysteresis measurement in Fig. 1 or in the electromechanical response in Fig. 2. We suspect that this arises from polarization switching at broad range of applied electric fields.

The broadening of each contribution to the x-ray reflection at increasing applied electric field, as shown in Fig. 3, is a second signature of the incomplete switching. Based on the Gaussian fits, we find that the full widths at half maximum (FWHM) of two components significantly increase from  $0.03^\circ$  and  $0.08^\circ$  at  $E=0$  to  $0.09^\circ$  and  $0.17^\circ$  at  $E=1.25$  MV/cm. If we interpret these widths as arising from the development of a distribution of the lattice constant across a range of values, we find that the lattice constants vary by up to  $0.03 \text{ \AA}$  within each peak. The width of the distribution of lattice constants in this case is similar to the maximum lattice distortion induced by the applied electric field.

A possible origin of broad distribution of lattice parameter under applied electric fields can be suggested by recent theoretical studies of the coercive fields of the individual components of superlattices [5]. It has been predicted for  $\text{BaTiO}_3/\text{SrTiO}_3$  [5] and  $\text{KNbO}_3/\text{KTaO}_3$  [9] superlattices, that the smaller polarization of the dielectric components is switched at a lower

coercive electric field with a relatively small increase in the depolarization energy, which is proportional to the square of remnant polarization [5]. We thus suggest the following model for the broadening observed in Fig. 3. When applied electric field reaches a value between the coercive fields of the two components of the superlattice, the polarization of  $\text{CaTiO}_3$  layers switches to have the same direction as the applied electric field, and the lattice constant of  $\text{CaTiO}_3$  layer increases due to the piezoelectric distortion. Meanwhile, polarization of  $\text{BaTiO}_3$  is not yet switched and the lattice parameter of  $\text{BaTiO}_3$  decreases with electric field. The average lattice parameter acquires broad range of values within the spot size of focused x-ray beam due to small local variations in the coercive fields.

## CONCLUSIONS

The structural and electrical response to applied electric fields are investigated in the ferroelectric/dielectric superlattices. A broadening of the distribution of the average lattice parameter of the superlattice is observed at applied electric fields larger than the coercive electric field derived from the polarization-electric field hysteresis measurement. The broadening is consistent with a model in which the constituent layers of superlattice have slightly different coercive electric fields, resulting in a wide variation of local piezoelectric properties.

## ACKNOWLEDGMENTS

This work was supported by the U.S. Department of Energy, Office of Basic Energy Sciences, through Contract No. DE-FG02-04ER46147. H.N.L. acknowledges support from the Division of Materials Science and Engineering U.S. Department of Energy, through Contract No. DE-AC05-00OR22725. Use of the Advanced Photon Source was supported by the U. S. Department of Energy, Office of Science, Office of Basic Energy Sciences, under Contract No. DE-AC02-06CH11357.

## REFERENCES

1. J. B. Neaton and K. M. Rabe, *Appl. Phys. Lett.* **82**, 1586 (2003).
2. H. N. Lee, H. M. Christen, M. F. Crishlom, C. M. Rouleau and D. H. Lowndes, *Nature* **433**, 395 (2005).
3. W. Tian, J. C. Jiang, X. Q. Pan, J. H. Haeni, Y. L. Li, L. Q. Chen, D. G. Schlom, J. B. Neaton, K. M. Rabe and Q. X. Jia, *Appl. Phys. Lett.* **89**, 092905 (2006).
4. V. A. Stephanovich, I. A. Lukyanchuk and M. G. Karkut, *Phys. Rev. Lett.* **94**, 047601 (2005).
5. S. Lisenkov, I. Ponomareva and L. Bellaiche, *Phys. Rev. B* **79**, 024101 (2009).
6. A. Grigoriev, R. Sichel, H. N. Lee, E. C. Landahl, B. Adams, E. M. Dufresne and P. G. Evans, *Phys. Rev. Lett.* **100**, 027604 (2008).
7. D. H. Do, A. Grigoriev, D. M. Kim, C. B. Eom, P. G. Evans and E. M. Dufresne, *Integr. Ferroelectr.* **101**, 174 (2008).

8. D. H. Do, PhD thesis, University of Wisconsin-Madison, 2006.
9. M. Sepliarsky, S. R. Phillpot, D. Wolf, M. G. Stachiotti and R. L. Migoni, J. Appl. Phys. **90**, 4509 (2001).